JOURNAL OF OPTOELECTRONICS AND ADVANCED MATERIALS Vol. 9, No. 5, May 2007, p. 1377 - 1381

Section 3. Nano and microstructured materials and thin films
Invited Paper

Strain influence on crystallography of $AgNbO_3$ – based thin films

MATJAZ VALANT*, ANNA-KARIN AXELSSON, BIN ZOU, NEIL ALFORD
London South Bank University, Centre for Physical Electronics and Materials, 103 Borough Road, SE1 0AA, London, UK

$AgNbO_3$ and $(Ag_{0.9}Li_{0.1})NbO_3$ thin films were grown on a $LaAlO_3$ (001) single crystal substrate by the PLD technique. A crystallographic analysis of the films showed on a high epitaxial relationship with the substrate. High roughness and texturing of the surface shows that the island-growth mechanism was involved during the deposition. A stress-induced distortion of the thin-film unit cell dominates over a substitutionally induced distortion, which was expected from a doping with Li. A high-energy clamping of the substrate and the films results in a significant uniform in-plane compressive macrostrain with a high concentration of structural defects concentrating on the interface. The defects cause a microstrain to be anisotropically distributed and larger along the in-plane direction.

(Received November 14, 2006; accepted April 12, 2007)

Keywords: $AgNbO_3$, Thin films, Pulsed laser deposition, Crystallographic properties

1. Introduction

A development of $AgNbO_3$-based materials was triggered by an unique combination of several physical characteristics of these materials; (i) an unusually high permittivity, (ii) modest dielectric losses (iii) a prospect for a low temperature dependence of the permittivity and (iv) a fairly low sintering temperature. Without much further adjustments the permittivity (400-600) and the dielectric losses (tanδ = $2\cdot10^{-4}$ at 1MHz, Q = 700 at 1 GHz) [1] are good enough for many kinds of passive applications, however, the temperature dependence of the permittivity on certain parts of the curve exceeds 1000 ppm/K. The majority of applied research on this material was focus in temperature stabilization of the permittivity, which resulted in achieving values below 50ppm/K.

Current research on the $AgNbO_3$-based systems is focused on thin and thick film synthesis and investigation of their dielectric properties and dielectric tuneability. The reasons that make this field of research attractive are various. The entire development of the electronic industry is shifting from bulk components to integrated devices based on thick or thin film technology, which is significantly cheaper in a mass production. In the case of the $AgNbO_3$-based films this is even more pronounced due to the lower material consumption of relatively expensive oxides. Preliminary studies on single crystals indicate that much better properties can be expected from the epitaxially grown films than from the bulk ceramics where the random grain orientation, and a presence of porosity and grain boundaries represent extrinsic factor that affect key properties adversely.

The initial work on tuneability of $AgNbO_3$-based films was peformed by Zimmermann et al., [2] on screen printed 3-6 μm thick films on Al_2O_3 substrate. They demonstrated fairly high tuneability of such films, which reached 19% (1.2 kV/mm) and 16% (1kV/mm) for $Ag(Nb_{0.8}Ta_{0.2})O_3$ and $Ag(Nb_{0.9}Ta_{0.1})O_3$ films, respectively. For possible applications in tuneable microwave devices, such as phase shifters, tuneable filters and varactors, these films were also characterized in the frequency range from 4 to 13GHz. The tuneability decreases with frequency to 5% at 4GHz and <1% at 13 GHz. This is accompanied with an increase in dielectric losses to tanδ~0.15 at 10 GHz. It is suggested that the reason for such behaviour is in the presence of a relaxation at around 30GHz, most probably due to phonon scattering effects.[3] If this problem is not overcome in the future the use of these thick films will be restricted to the low-GHz applications.

Telli in his doctoral thesis [4] reported on successful formation of epitaxial thin films by spin-coating of $AgNbO_3$ chemical solutions on (001)$LaAlO_3$ and (001)$SrRuO_3$/(001)$LaAlO_3$ (SRO/LAO) substrates. A tuneability of 21.4% was measured for bias of 190kV/cm. He noticed that for $AgNbO_3$ on the SRO/LAO substrate the phase-transition sequence completely changes. No detailed analysis of the observed phase-transition sequence was performed but the effect results in a remarkable deviation of the room-temperature permittivity of the thin film (ε_r=550) from values typical for the bulk (ε_r=120). Nevertheless, the thin films retained moderate dielectric losses, which is very important for possible applications.

Koh and Grishin [5] synthesized and characterized $Ag(Nb_{0.62}Ta_{0.38})O_3$ thin films deposited on $LaAlO_3$. Crystallographic analyses showed that the film exhibited very high c-axis orientation (001) of the prototype unit cell with strictly a cube-on-cube epitaxial relationship. The characterization of the thin films was mainly oriented into their possible application in tuneable devices. The tuneability was measured to be 16.8% at 200kV/cm. At the same time the dielectric losses were rather low, tanδ=0.0033 (at 1MHz). The permittivity was determined to be 224 (at 1kHz). The performance of the

$Ag(Nb_{0.62}Ta_{0.38})O_3$ film deposited on the $LaAlO_3$ surpass the performances of $(Ba,Sr)TiO_3$, which today is regarded as a prime candidate for the electrically tuneable devices. Taking into account that not much work has been done so far on an optimization of these characteristics of the $Ag(Nb,Ta)O_3$ thin films we can expect even further improvements and serious consideration of these materials in commercial tuneable devices.

During a deposition of thin films a stress is generated in the films, which can cause a significant change in the crystal structure of the material and, consequently, in its functional properties. A particular type of the crystal-structure distortion will influence the functional properties in a similar way, whether it is induced by an introduction of a foreign ion or by generation of stress/strain. With this study we aimed to understand a magnitude of the distortion imposed by the ion substitution compared to that imposed by the stress generated during the film deposition. A crystallographic analysis of doped and Li-doped $AgNbO_3$ in a form of bulk and PLD thin films will be perfomed and used to comperatively evaluate these two effects.

2. Experimental

A 248 nm KrF excimer laser was used to ablate a stoichiometric $AgNbO_3$ target. The films were grown on a single-crystal 001 $LaAlO_3$ substrate. The processing conditions were: target to substrate distance 70mm, oxygen pressure in the chamber 0.5bar, substrate temperature 550ºC, laser beam energy 520 mJ and annealing time 20 min. Film thickness was measured using Dektak 6M Stylus profiler.

The crystallographic analysis was performed with high-resolution x-ray diffractometer Philips Xpert Pro using Cu source with line focus, x-ray mirror, Ge monochromator and sealed proportional counter or X'celerator detector for high speed data collection. An orientational relationship between the films and the substrate was determined by a phi scan on (103) planes. Diffraction conditions for the phi scan were $2\Theta=76.7033^o$ and $\omega=18.4000^o$ for $AgNbO_3$, and $2\Theta=79.2119^o$ and $\omega=18.4349^o$ for $LaAlO_3$. An out-of-plane unit cell parameter (c-axis) of the film was calculated from a 2Θ-Θ scan while both in-plane parameters (a- and b-axis) were determined from a grazing-incidence scan. Microstrain was calculated from the same scans using the Sherrer's formula. A broadening of the peaks was determined by measuring FWHM of the peaks. A rocking curve (ω-scan) on (002) planes and atomic force microscope were used to obtain information about topography of the film surface.

3. Results and discussion

According to work of Schiau et al. [6] $AgNbO_3$ at room temperature is described with an orthorhombic unit cell, a Pbcm space group and cell parameters a=5.5468Å b=5.6038Å and c=15.642Å. A slight off-centering of Nb ions and tilting of oxygen octahedra are the reasons why an underlaying monoclinic cell must be translated into much bigger orthorhombic cell. The translation matrix between the Pbcm orthorhombic cell and the P2/m monoclinic cell is {1 0 1, 0 4 0, -1 0 1} and the cell parameters are in a relation $a=\sqrt{2}\,a_p$, $b=\sqrt{2}\,b_p$ and $c=4c_p$. In our study we will described the structure of $AgNbO_3$ with the underlaying monoclinic cell. By this we do lose information about the commensurate ordering, which in x-ray diffraction pattern results in an appearance of faint diffraction lines. However, an investigation of these details in the thin film is above a detection limit of the analytical methods that we want to apply and, therefore, the simplification of the crystallographic system comes without affecting the final results.

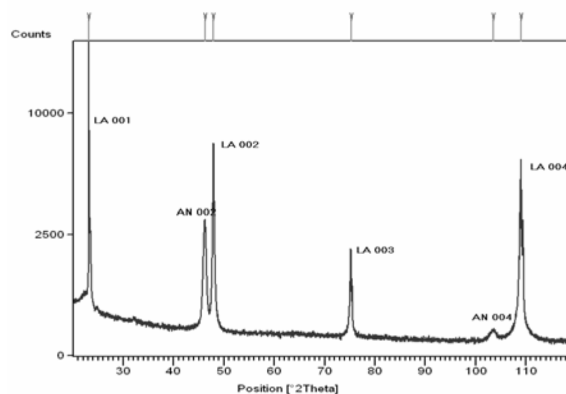

Fig. 1. XRD 2Θ-Θ scan of a $AgNbO_3$ 200nm thin film pulsed-laser deposited on a $LaAlO_3$ (001) single crystal substrate.

Fig. 1 shows a 2Θ-Θ scan of the $AgNbO_3$ thin film deposited on $LaAlO_3$. In addition to a (00*l*) family of $LaAlO_3$ diffraction lines two $AgNbO_3$ lines can be observed, (002) and (004). No intensity can be found for (001) and (003) planes. Formally these diffractions are not extinct in the P2/m space group but a theoretical calculation of the $AgNbO_3$ diffraction pattern confirms our experimental observation regarding the zero intensity of (001) and (003) lines. The presence of only (00*l*) diffraction lines of $AgNbO_3$ indicates on a high level of epitaxy between the film and the substrate. Ultimately this was confirmed with a phi scan on a plane oblique to the film/substrate interface. A four-fold symmetrical (103) plane was selected and the phi scan showed a perfect angular coincidence between the substrate and the film (Fig. 2). No other peaks in the phi scan can be detected what confirms that the film grows in a cube-on-cube epitaxial relationship with the substrate.

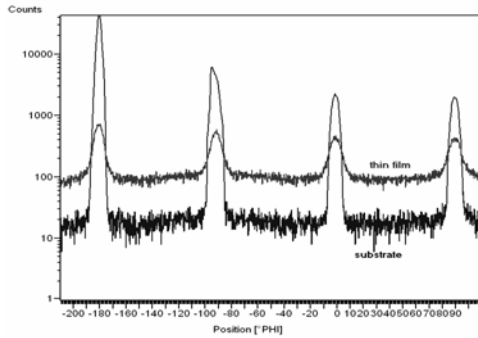

Fig. 2. XRD phi scan of an off-normal (103) planes measured at oblique geometry.

As only two diffraction lines are available for a calculation of a particular unit-cell parameter the calculation is necessarily imprecise. From a derivative of Bragg equation, $\Delta d/d \approx \cot\Theta \times \Delta\Theta$, can be seen that the error tends to zero when Θ approaches 90°. To decrease the error the values, calculated from positions of the available diffraction lines, were extrapolated towards $\Theta=90^o$ using Nelson Riley formula.

$$F(\Theta) = \frac{\cos^2\Theta}{\sin\Theta} + \frac{\cos^2\Theta}{\Theta} \tag{1}$$

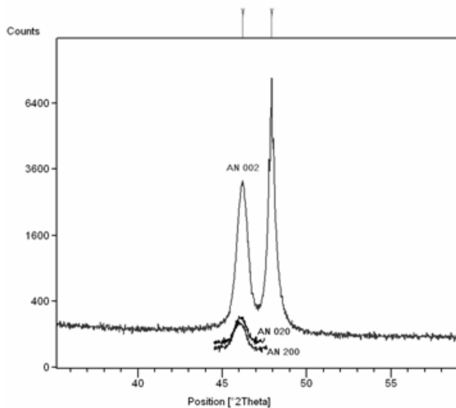

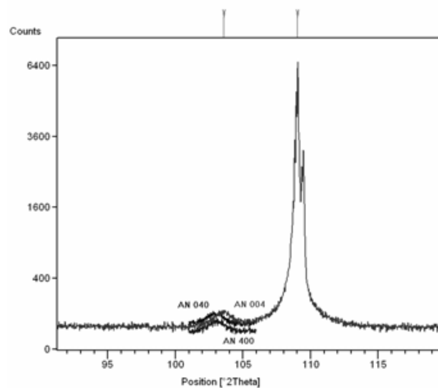

Fig. 3. XRD 2Θ-Θ scan on (002) planes and grazing-incidence diffraction on (020), (200), (040) and (400) planes

The cell parameters for the $AgNbO_3$ film determined from Fig. 3 are: a=3.933(1) Å, b=3.936(1) Å and c=3.925(1) Å. If these parameters are compared with the parameters, determined for a $AgNbO_3$ single crystal by Schiau et al. (a=3.9222 Å, b=3.9625 Å, c=3.9105 Å) [6], it can be seen that the b-axis is significantly compressed to accommodate to the cubic template of the $LaAlO_3$ substrate. This strain is compensated by a slight increase of the other two axes; however, the unit-cell volume is still reduced from 60.776 $Å^3$ to 60.755 $Å^3$. This shows that the film is under a significant uniform compressive stress imposed by the $LaAlO_3$ substrate with the smaller unit cell (3.821 Å).

In addition to the macrostrain, which is caused by uniformly distributed compressive or tensile stress and results in a shift in a position of diffraction lines, we also have analyzed microstrain. The microstrain comes from a non-uniform distribution of stress mainly due to a presence of dislocations and point defects. Such stress locally changes ionic distances within a unit cell and results in broadening of diffraction line around an original position. To calculate a level of microstrain from the width of the diffraction line we used the Sherrer's formula

$$\beta_t^2 = \left\{\frac{0.9\lambda}{D\cos\Theta}\right\}^2 + \left\{4\varepsilon\tan\Theta\right\} + \beta_0^2 \tag{2}$$

where β_t is broadening of the diffraction line, D crystallite size, ε microstrain and β_0 instrumental broadening (0.05^o). There is no contribution of the crystallite size to the total line broadening along a- and b-axis directions of the thin film. For a c-axis direction D represents a thickness of the film and its contribution to the line broadening becomes important only when the thickness is smaller then 100nm. For our 200 nm thick films this contribution is negligible and the broadening comes only from the microstrain. The measured microstrain for the $AgNbO_3$ film in the out-of-plane direction was 0.51% while in the in-plane directions 0.75% and 0.69%. As the results show the microstrain is aniosotropic and much higher along the in-plane directions. This is a consequence of a high-energy interfacial clamping, which is obvious from the macrostrain measurement. A lattice mismatch of the substrate and the film is locally relaxed with a creation of dislocations and this contributes to the increased in-plane microstrain.

A topography of the film surface was investigated to gather information about roughness and texturing, which helped us in estimating a growth mechanism. The layer-growth mechanism usually results in less rough and less textured surface as the island-growth mechanism and is, therefore, preferred.

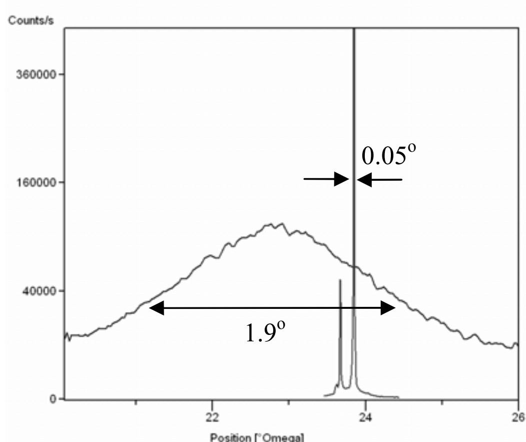

Fig. 4. XRD rocking curve on (002) planes of a $AgNbO_3$ film and a $LaAlO_3$ substrate.

A rocking curve taken on (002) planes of the thin film show a massive broadening of the peak with FWHM of 1.9° indicating a high degree of texturing (Fig. 4). The $LaAlO_3$ peak shows broadening of only 0.05°, which is characteristic for single-crystal surfaces. Two $LaAlO_3$ peaks can be observed because of an imminent twinning in the single crystal. The high texturing and roughness of the thin film was confirmed with AFM investigations. From the AFM analyzes we can calculate roughness (R_a) that is defined as an arithmetic average of the absolute values of the surface height deviation measured from the mean plane. The calculated R_a for the $AgNbO_3$ film was 30nm. The high texturing and the topography of the surface (Fig. 5) strongly indicate on the island-growth mechanism.

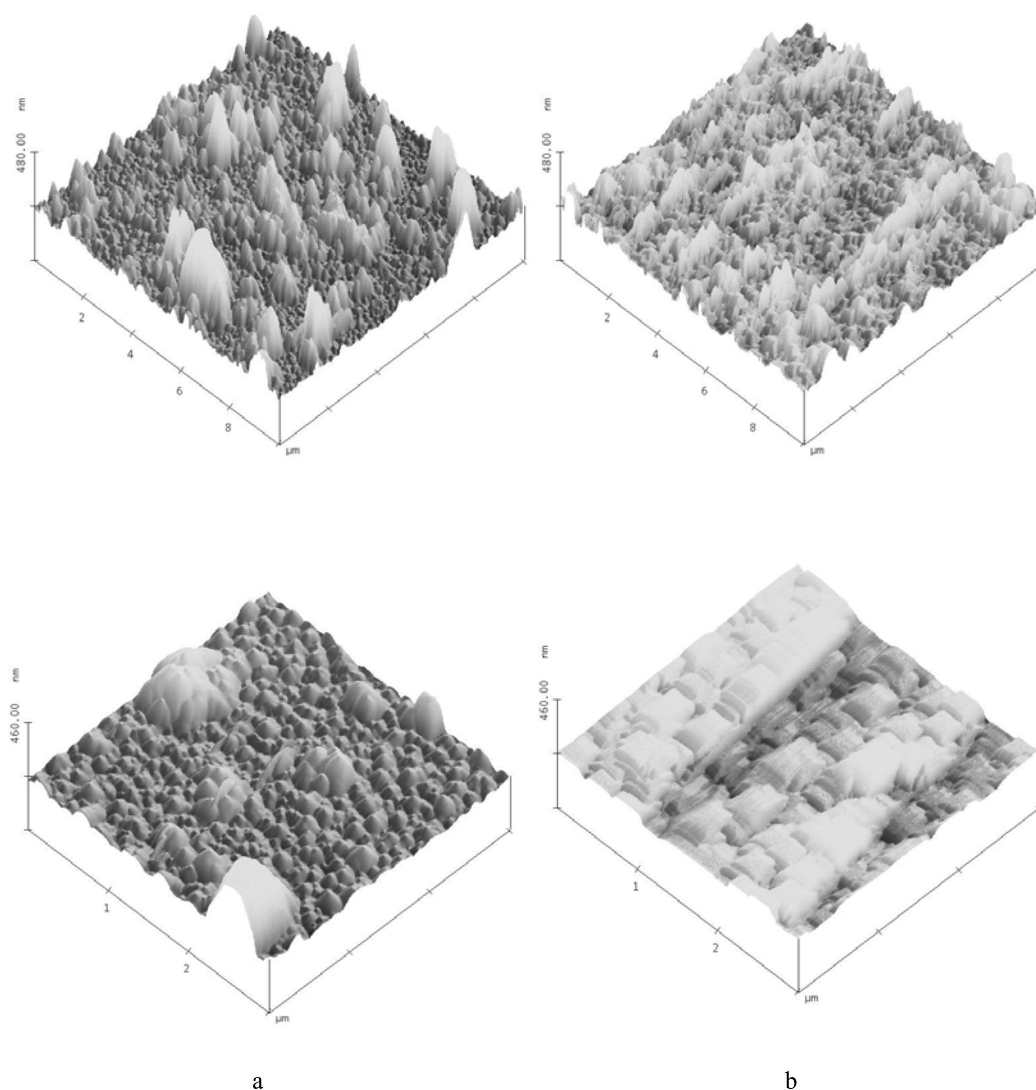

Fig. 5. AFM images of the surface of (a) $AgNbO_3$ and (b) $(Ag_{0.9}Li_{0.1})NbO_3$ films pulsed-laser deposited on $LaAlO_3$ (001) substrate.

An analogues set of analysis as for the $AgNbO_3$ film was performed for a Li-doped $AgNbO_3$ film with a stoichiometry of $(Ag_{0.9}Li_{0.1})NbO_3$. Results of the analysis are compared in Table I. Determined unit-cell parameters for $(Ag_{0.9}Li_{0.1})NbO_3$ film are very similar to those for the $AgNbO_3$ films despite the fact that Li^+ ion is much smaller then Ag^+. For a coordination number 8 (the data for coordination number 12 are not available) the ionic radius for Li^+ is 0.92 Å and for Ag^+ is 1.28 Å. [7] Only a small decrease in volume can be detected for the Li-doped thin film. The similar unit-cell parameters indicate that the stress-induced distortion of the unit cell dominates over the substitutionally induced distortion. The microstrain along the in-plane directions is higher then for $AgNbO_3$ but the microstrain along the out-of-plane direction is very much the same. These data suggest on different clamping conditions on the interface but similar concentration of point defects within the thin film crystal. Similar to the $AgNbO_3$ film the high roughness (R_a=20nm) and texturing of the thin-film surface shows on the island-growth mechanism.

Table 1. The results of the XRD analysis of $AgNbO_3$ and $(Ag_{0.9}Li_{0.1})NbO_3$ thin films pulse-laser deposited on a $LaAlO_3$ (001) single-crystal substrate.

Composition	a (Å)	b (Å)	c (Å)	V (Å^3)	ε_a(%)	ε_b (%)	ε_c (%)	Rocking curve width (^{o})
$AgNbO_3$	3.933	3.936	3.925	60.755	0.75	0.69	0.51	1.9
$(Ag_{0.9}Li_{0.1})NbO_3$	3.932	3.933	3.927	60.743	0.95	0.93	0.56	2.1

4. Summary

Highly epitaxial $AgNbO_3$ and $(Ag_{0.9}Li_{0.1})NbO_3$ PLD thin films were grown on a $LaAlO_3$ substrate. A crystal structure of the films accommodates to the cubic template of the substrate resulting in a compressive stress on the film. A stress-induced distortion of the unit cell dominates over a substitutionally induced distortion, which was expected from the doping with Li. Microstrain, developed during the deposition, is aniosotropic. It is higher along in-plane directions, which is related to a high-energy interfacial clamping. Similar out-of-plane microstrain for the $AgNbO_3$ and $(Ag_{0.9}Li_{0.1})NbO_3$ thin films is showing on a similar concentration of point defects within the thin-film crystal. Topographical studies indicates the island-growth mechanism.

The described characterisation of the thin films represents a basis for further studies that will involve investigation of an influence of deposition conditions on a growth mechanism, an influence of a stress relaxation and oxygen annealing on structural characteristics (micro- and macrostrain), and functional properties (ferro and piezoelectric properties, tuneability) as a function of stress and topography.

References

[1] M. Valant, D. Suvorov, C. Hoffmann, H. Sommariva, J. Europ. Ceram Soc. **21**(15), 2647 (2001).
[2] F. Zimmermann, W. Menesklou, E. Ivers-Tiffee, Integrated Ferroelectrics **50**, 181 (2002).
[3] R. Schwab, R. Sporl, J. Burbach, J. Heidinger, F. Koniger, Display and Vacuum Electronics, ITG-Fachber., VDE-Verlag **150**, 363, (1998).
[4] M. B. Telli, M.B., Doctoral thesis, The Pennsylvania State University, USA, 2005
[5] J.H. Koh, A. Grishin, Appl. Phys. Letters **79**(14), 2234, (2001).
[6] P. Sciau, A. Kania, B. Dkhil, E. Suard, A. Ratuszna, J. Phys. - Condensed Matter **16**(16), 2795 (2004).
[7] R. D. Shannon, Acta Cryst. **A32**, 751 (1976).

*Corresponding author: valantm@lsbu.ac.uk

.